The Effect of Groundwater Inflow on Evaporation from a Saline Lake

JEFFREY M. WHITING

Saskatchewan Research Council, Saskatoon, Saskatchewan, Canada S7N 0X1

(Manuscript received 7 March 1983, in final form 24 September 1983)

ABSTRACT

A decade study of the hydrometeorology of Big Quill Lake in Saskatchewan, a saline prairie lake, has effectively used remote sensing to delineate groundwater inflow. The lake covers an area of 250 square kilometers with the groundwater seeping through 4 square kilometers. The salinity of the lake water forces the fresher groundwater to the surface by convection and spreads the colder groundwater by diffusion over an area of 50 square kilometers. The magnitude, source and discharge rate were determined using thermal diffusivity from data supplied by thermal infrared line scanning. Two thermal scans were made of the lake and the data extended to provide a seasonal index using LANDSAT computer compatible tapes. The seasonal thermal index was extended further using four shore-based climatological stations to provide areal evaporation using a modified Penman equation and a diffusion equation.

1. Introduction

Hydrometeorological phenomena are dynamic so their comprehensive and prediction are both difficult and challenging. They contain cyclic components ranging from diurnal to climatic trends. Predicting the magnitude and recurrence intervals is the aim of the research which was conducted on Big Quill Lake (Fig. 1). Big Quill Lake is at the center of an internal drainage system of surface water and is situated in an Aspen Parkland natural vegetation zone. The lake is very shallow–its depth does not exceed 3 m (Fig. 2)—and yet it is relatively large (250 km^2). The area of its internal drainage basin is approximately 2700 km^2. The water of the lake is saline, reaching a concentration of 81 000 mg/L^{-1} below the ice in winter. The dissolved solids are mainly sodium and magnesium sulphates.

The decade-long study has shown that groundwater is an important component in the hydrological balance of the lake and that the water entering the lake is a persistent but not a continuous discharge. By various methods, the groundwater inflow has been estimated to be as high as 30% of the lake water which is lost annually by evaporation (Whiting, 1977).

If the groundwater flowing into the lake is from a relatively deep aquifer, then the seep will have a constant temperature (McLin *et al.*, 1975). This constant temperature source creates an error in the calculation of evaporation if not incorporated into the lake temperature. The magnitude of the error depends upon the size of a surface anomaly caused by the bottom groundwater seep. The size of the anomaly is dependent upon the discharge rate. With a lake this large, sustained winds will generate substantial wave action causing rapid mixing, which further increases measurement errors.

In order to determine the amount of water discharged annually from the aquifers beneath the lake, the location of the aquifers and the seeps must be known. A drilling survey, conducted between 1966 and 1969, indicated in a general way that the local aquifer must be integrated into a complex regional system and also connected to a buried pre-glacial river valley passing through three provinces. These local aquifers probably underlie only the southern half of the lake.

This paper is concerned with the determination of the size of the surface anomaly attributed to groundwater and the discharge volume. Using infrared (IR) thermal temperatures and surface measurements, areal evaporation is calculated, and the error due to the temperature difference between the groundwater and the open water is derived. The method is hypothetically extended using scanner data from the green–yellow color band of the LANDSAT satellite.

2. Source of data

A temperature map (Fig. 3a) was constructed, using an analog computer at the Canada Centre for Remote Sensing (CCRS) in Ottawa, which selectively density sliced only the water areas from the thermal infrared scanner data. This represented one third of the full scale of six possible levels. The scan lines were calibrated using an onboard PRT-5 in conjunction with a photometer along the nadir trace line to give additional calibration data between flight lines. The airborne thermal scanning was flown at an altitude of 3800 m above sea level. Five lines were flown over the lake on 30 June 1974. The resolution of data is ±1.8 m. A preliminary flight was made 15 July 1973, at 6700 m above the sea level but with a resolution of

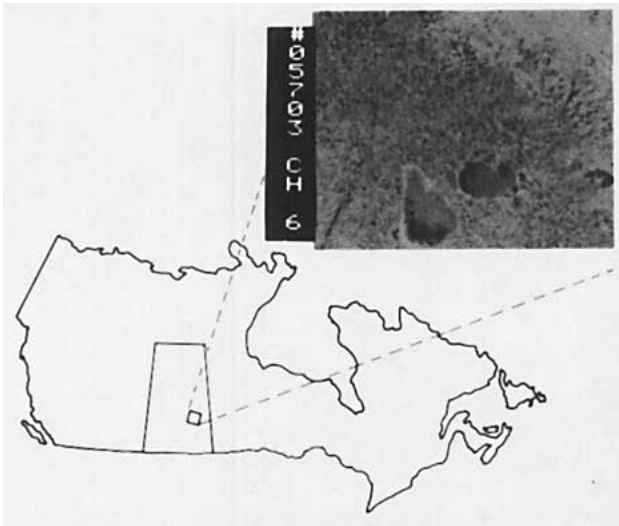

FIG. 1. Location of Quill Lakes using LANDSAT-1 (MSS 2) Saskatchewan, Canada.

only ±200 m. The 1973 equipment used could not produce the six-level density tapes. The map shows the same nine groundwater inflow areas which can be inferred from LANDSAT digital data (Fig. 3b) on computer compatible tapes (CCT) and airborne radio-wave phase detection of subsurface resistivity profiles (E-PHASE) (Whiting, 1976).

The LANDSAT satellite, at an altitude of 920 km, broadcasts data to Prince Albert (PASS) in Canada using information supplied by the United States National Aeronautics and Space Administration (NASA). The analog reception tapes are sent to Ottawa and translated into digital tapes. The tapes (CCT) contain 2400 scan lines. Each scan line consists of 3600 pixels. A pixel represents the reflected light intensity of a ground area of approximately 60 × 90 m. The light intensity is divided into 64 digital steps. Each letter in Fig. 3b covers an area of approximately 150 × 180 m (with A–Z representing 1–26 reflectivity steps and 1–9 and 0 representing 27–36 and 37; the remaining 27 steps are not used).

The tenth anomaly (10 in Fig. 3b) is caused by dynamic coupling to atmospheric events (Whiting, 1976). In 24 satellite images examined, this anomaly was not always present. When present the intensity distribution from cross correlation between the green–yellow color band (Multi Spectral Scanner Band 1, MSS 1) and red band (MSS 2) always had two nodes, whereas the remaining nine anomalies are only binodal when atmospheric disturbances occur.

3. Data analysis

The infrared and LANDSAT data provide either temperature values or reflected radiant intensity and their distributions. It was originally hoped to produce a two-dimensional, steady state heat flow solution which would yield the volumetric flow of the groundwater seeps. The primary obstacles to this approach were 1) a lack of knowledge of the critical third dimension: vertical movement, 2) a lack of ground measurements and 3) a lack of calibration between IR and MSS 1.

Freshwater discharging from the bottom of a saline lake will rise to the surface by density buoyancy and then spread out on the surface due to the slope of the anomaly (Lee, 1969). When there is a difference in temperature between the groundwater and the lake, the area of thermal contrast can be seen on the IR imagery. The lake or groundwater temperature will not affect the density buoyancy due to the large density difference between the seep and the lake (i.e., the seep water is always more buoyant). The size of this thermal anomaly and the degree of thermal contrast depends upon the volumetric discharge and dispersion by wind. In order to determine hypothetically the volume of the discharge from imagery alone, an empirical correlation from Lee (1969) was used (Fig. 4). The area of the temperature anomalies of annuli (such as 2) in Fig. 3a were measured by taking the length and width

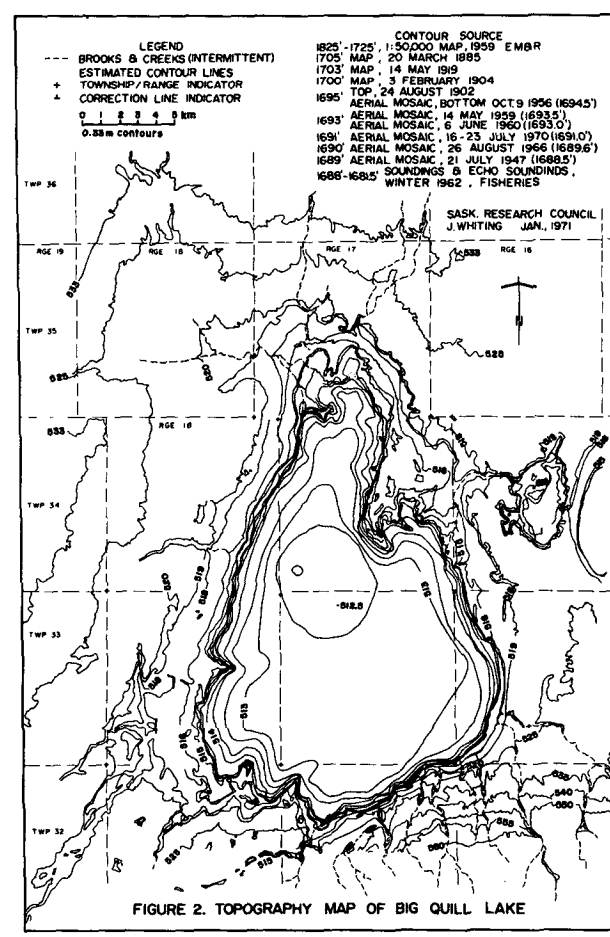

FIG. 2. Topography map of Big Quill Lake.

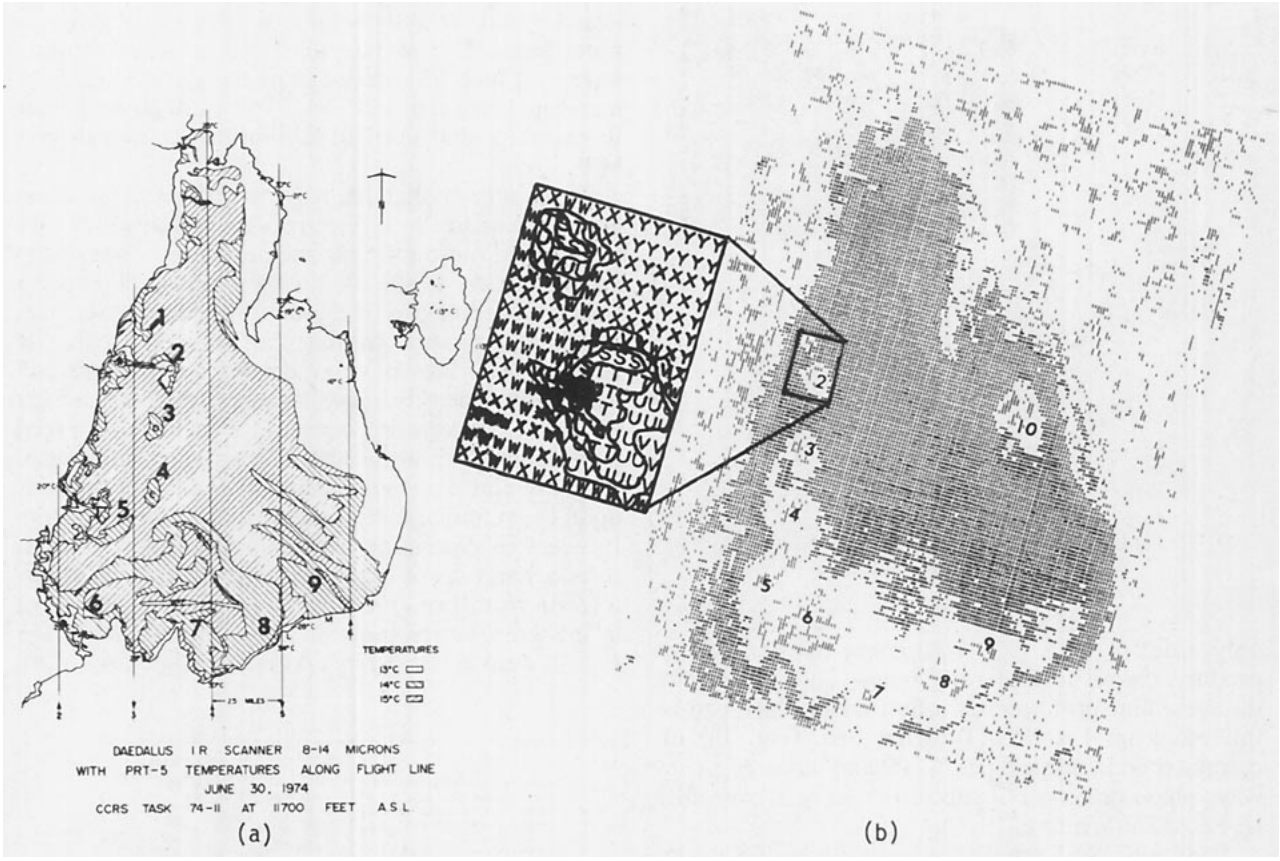

FIG. 3. Infrared scanning shows similar anomalies as the LANDSAT-1, 4 September 1973: (a) infrared interpretation, (b) digital LANDSAT image.

of each contour line around the anomaly and using the area of an ellipse in the formula below. The thermal anomaly may be expressed as

Thermal Anomaly:

$$TA = \sum_{i=1}^{n} A_i \left(T_n - \frac{T_i + T_{i-1}}{2} \right), \qquad (1)$$

where TA is in °C m^2, A in m^2 and T in °C.

The results are shown in Table 1a. Lee (1969) used the combined influence of air temperature, groundwater supply temperature and lake surface temperature to calibrate the discharge volume (V) as follows:

$$V = TA \times K, \qquad (2)$$

where

$$K = [a(T_n - T_A) + b(T_n - T_a)]. \qquad (3)$$

Here T_n is open water temperature (°C), T_a the groundwater temperature (=6°C) and T_A the air temperature (°C). The coefficients are

$$a \approx \begin{cases} 4, & \text{when } T_n - T_A > 0 \\ 8, & \text{when } T_n - T_A < 0, \end{cases}$$

$$b \approx \begin{cases} 1, & \text{when } T_n - T_a > 0 \\ 2, & \text{when } T_n - T_a < 0. \end{cases}$$

The anomaly (V) has maximum contrast (development) when both T_a and T_A are lower than T_n since K is inversely proportional to the magnitude of the thermal anomaly for a given V. If the difference in

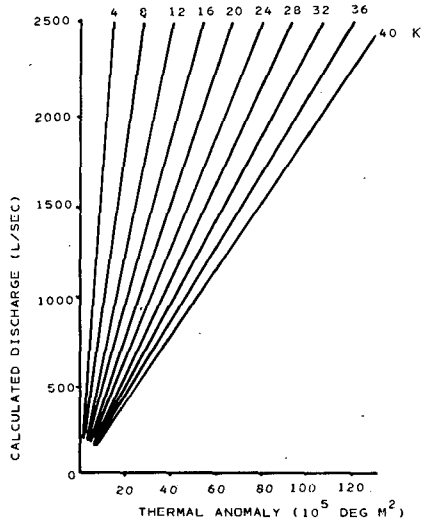

FIG. 4. Nomogram for calculating thermal anomaly and K.

TABLE 1. Calculation of groundwater inflow volumes, 1973.

Units location	Number of rings	Area (10^5 m^2)	Temperature anomaly (10^6 m^2 °C)	Volume (L s^{-1})
		(a) Survey—30 June Infrared		
1	1	6.5	94	2068
2	2	17.4	157	3454
			41	902
3 (C)	1	8.5	122	2684
4 (D)	1	9.0	130	2860
5 (E)	1	67.9	868	19 096
6	1	45.0	648	14 256
7		50.0	—	—
8	1	70.6	—	—
9		58.0	—	—
Total		333.9		(85 014)*
Rate spread out over lake		2500		(6600)*
		(b) LANDSAT—4 September Radiant energy (10^5 mW cm^{-2} m^2)		
1	4	4.1	22.6	—
2	4	15.4	56.8	—
3	5	26.2	45.7	—
4	6	50.0	102.1	—
5	7	79.7	173.9	—
6	4	54.3	164.4	—
7	3	10.3	34.1	—
8	3	16.7	44.5	—
9	3	11.1	44.3	—
Total		267.8	688.2	—
Rate spread out over lake		2500		6666†
		(c) LANDSAT—5 September (10^5 mW cm^{-2} m^2)		
1	3	2.7	7.8	—
2	3	15.4	28.0	—
3	2	13.8	32.0	—
4	4	21.1	47.5	—
5	4	34.3	63.8	—
6	3	31.6	83.2	—
7	1	3.5	58.5	—
8	2	11.9	26.1	—
9	2	2.4	12.9	—
Total		136.6	301.6	—
Rate spread out over lake		2500		5720†
		(d) 24 LANDSAT images (1973–75)		
1		4.4	63	1386
2		13	141	3102
3		10	144	3168
4		19	274	6028
5		92	1178	25 916
6		49	706	15 523
7		20	224	4928
8		21	302	6644
9		26	562	6182
Total		254.4	3594	72 877
				7404
1968–75 mean annual [using Lake balance (Whiting, 1977)] (L s^{-1})				7380
30 year mean annual [using Lake balance (Whiting, 1977)] (L s^{-1})				6900

* Including 7–9 which are not complete anomalies (Annuli).
† Estimated using comparison to IR and reduced by ratio of the number of rings.

temperature were the same but with both T_a and T_A warmer than T_n, then the anomaly would be half as large. The optimum time for the IR survey would be pre-dawn in late spring or fall when $T_A < T_a$ or $T_a < T_n$.

The same procedure to calculate *TA* [Eq. (1)] was used with the LANDSAT CCT's (Table 1b–d) where temperature was replaced by radiant energy. A comparison was made between each LANDSAT band and the IR anomalies. The best results were obtained with MSS 1 (Fig. 3b). Researchers have found that MSS 1 shows lake dynamics due to deeper penetration into the water, while MSS 2 shows turbidity and MSS 3 and 4 show chlorophyl *a* (Bukata and Bruton, 1974). The groundwater inflow causes a change in reflected radiant energy. The radiant energy calibration values for LANDSAT data were obtained from Otterman and Fraser (1976). The air temperatures for the calculation of K were obtained from four climatological sites around the lake. Water temperatures were calculated by using a regression equation (Whiting, 1977) based upon three hydrometeorological stations:

$$T_n = T_A + 3.3 \quad \text{(Notations given previously).} \quad (4)$$

During the period 1973–75, 24 cloud free summer LANDSAT images were obtained. Of these, 4 and 5 September 1973 images were chosen for detailed analysis (Table 1b, c). Two consecutive days were chosen to ensure that the answers were compatible not only with the IR values but also with each other. The groundwater discharge between consecutive days is assumed not to vary. Data taken on consecutive days which are different by more than 10% are considered to be in error. Errors greater than 10% would not give an improvement in calculation accuracy over standard methods.

The wind on 30 June (<5 m s^{-1}) produced a hydrodynamically smooth boundary layer; on 4 and 5 September, the wind was above a velocity of 7 m s^{-1} needed to create surface tension instability. On 4 September, breaking waves were produced when the wind was between 11.6 and 14.3 m s^{-1} during the hour of the overpass. Water droplets above the air–water interface would not be attained (Banks, 1975). It is hypothesized that the increased area of the seeps in September are the result of wind. In the 4 September image, 3–7 rings or annuli (Table 1b) were present while on 5 September, 1–4 and on 30 June, only 1–2. The anomalies were therefore normalized by dividing *TA* by the number of rings for each seepage.

The increase in area caused by the wind is created by an induced surface current (q) (Wu, 1973)

$$q = \alpha U, \quad (5)$$

where α is a coefficient and U the 10 m wind (m s^{-1}).

Therefore, the area is increased by 8.5% with a wind of 5 m s^{-1}, 20% at 10 m s^{-1} and 33% at 15 m s^{-1}. This method provides a quantitative number to check the above normalizing method. But the data is derived on the hour (not during the time of overflight) and not over the lake. With SAR (radar), such as from SEASAT data, better wave and wind patterns could be attained. For the purpose of this paper, normalization based upon observed rings was used.

The estimated inflow was calculated by comparing the LANDSAT reflected radiance to infrared "*TA*" for 30 June 1973. The 4 September values have a ratio of 4 to 1 while 5 September values correspond to 7 to 1 (Fig. 5). The *TA* value was reduced by the ratio of the average number of rings on the satellite dates to that of the IR. Anomalies from 24 summer images were also estimated using average summer temperatures (Table 1d). The higher values were plotted in Fig. 5 against the 4 September values. The values tend to agree with the ratio of 7 to 1 on 5 September. The flows from specific days and the average flow from the groundwater seeps would indicate a continuous steady flow. The calculated long-term groundwater flow by the water balance method confirms this result (bottom of Table 1).

The temperature anomaly map (Fig. 3a) shows shore seeps as another source of groundwater. This source would be expected to be more variable. The near-shore anomalies can again be used to calculate volume flow. The MSS satellite data could not be used due to complicated radiant returns as a result of the shallow water. With the new thematic mapper data (from LANDSAT-4, band TM-1), this data may be obtained.

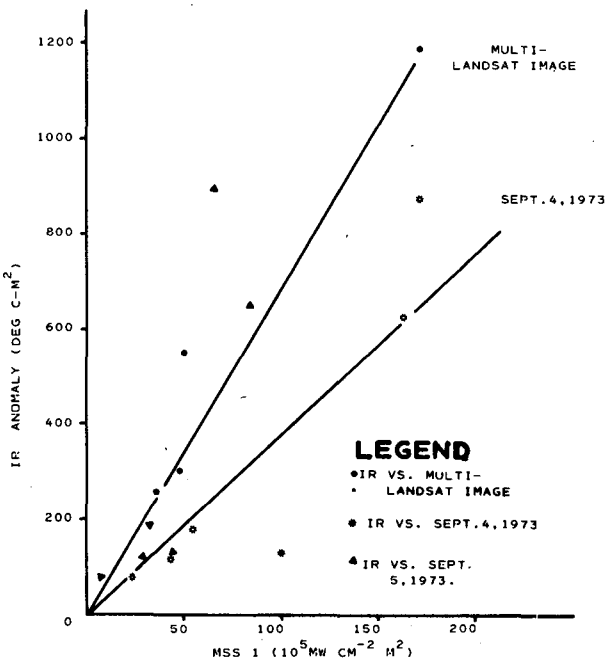

FIG. 5. Comparison between infrared and LANDSAT observations.

4. Evaporation calculations

The offshore groundwater seeps are considered to be the most important because they are a constant source of cold water. Two equations have been used to calculate evaporation: Penman (1948) and mass transfer (Lakshman, 1972).

Penman:

$$E = \frac{\Delta Q_{\text{net}} + 0.27EA}{[25.4(\Delta + 0.27)]}, \quad (6)$$

where

$$EA = 0.40(e_s - e_A)(1.0 + 0.076U) \text{ mb}$$

$$Q_{\text{net}} = 0.950Q_i - 5.67T_w^4 \times 10^2$$

Δ vapor pressure gradient
U wind at 10 m (mm day^{-1})
E evaporation (inches per day)
Q_i all wave radiation—measured (mW cm^{-2})
T_w temperature of water—measured (°C)
e_S, e_A vapor pressure at saturation and air (mb) respectively.

Mass transfer:

$$E = NU_2^{0.8}(e_S - e_A), \quad (7)$$

where

$U_2 = U_{10}^{0.2^{0.1429}}$ 2 meter wind derived from 10 meter (m s^{-1})

$$N = 0.184 \times 10^{-4} = f(m)\Phi(\delta)(P/A)$$

$f(m)$ wind profile power law function
$\Phi(\delta)$ boundary layer
P perimeter (m)
A area (m^2).

Calculations for 30 June (Table 2) give a difference between the hydrometerological site evaporation and the IR survey of 10 and 8% for the Penman and mass transfer respectively. As the difference between the constant groundwater temperature and the lake temperature increases, the error in the evaporation will increase. The shallow salt lake heats quickly and a gradient of 6°C m^{-1} is not uncommon. The maximum evaporation rate occurs in late August or early September. The evaporation error at this time, caused by the groundwater, is estimated to be 30%.

Based upon the 24 LANDSAT analyses, areal evaporation indices for three times of the year are shown in Fig. 6.

4. Conclusion

A number of remote sensing measurement and empirical relationships have been used to describe an extremely complex mixing problem. The methods described to estimate the groundwater flow in the paper have produced consistent results (5.8% variation to the 30-year mean water balance). The difference between groundwater flow estimates was 6.5%.

The groundwater inflow into Big Quill Lake is separated into two components: deep groundwater seepage, some distance off-shore and a near-shore seepage. The offshore seeps are a constant and continuous flow at a constant temperature. The flow of the near-shore seepage is widely variable and much smaller.

The greatest error in the evaporation calculation occurs when the open water and air temperatures are greatly different from the offshore groundwater temperature. The difference in temperature would be expected to occur for the greater part of the day and most of the summer. Hence, the degree of uncertainty in the lake balance calculation can be decreased with part of the groundwater now being determined to be constant. The error in evaporation, if the groundwater temperature is not taken into account, would be up to 34%.

The differences in area evaporation rates (using Penman and mass transfer equations) show the relative importance of wind factors. A simple area normalization procedure to account for dispersion by wind waves was used. The error of wind normalizing was checked using an empirical formula by Wu (1973). The degree of atmospheric coupling can also be determined by cross-correlation techniques.

Significant errors can result in lake evaporation calculation if the effect of temperature variation due to

TABLE 2. Evaporation calculation (cm day^{-1}) for 30 June 1973.

Time (CST)	Air temperature (°C)	Evaporation Penman			Mass transfer		
		(13°C)	(14°C)	(15°C)	(13°C)	(14°C)	(15°C)
1000	20.8	0.188	0.226	0.259	0.107	0.137	0.168
1100	21.9	0.185	0.221	0.221	0.096	0.127	0.158
1200	22.5	0.173	0.210	0.259	0.081	0.112	0.142
1300	*22.9*	*0.193*	*0.229*	*0.267*	*0.101*	*0.132*	*0.163*
Average	22.0	0.185	0.221	0.259	0.096	0.127	0.157
Area apportionment*		*0.005*	*0.073*	*0.158*	*0.003*	*0.046*	*0.096*
Total (cm day^{-1})				0.236			0.145

* Average evaporation is multiplied by the apportionment of area affected.

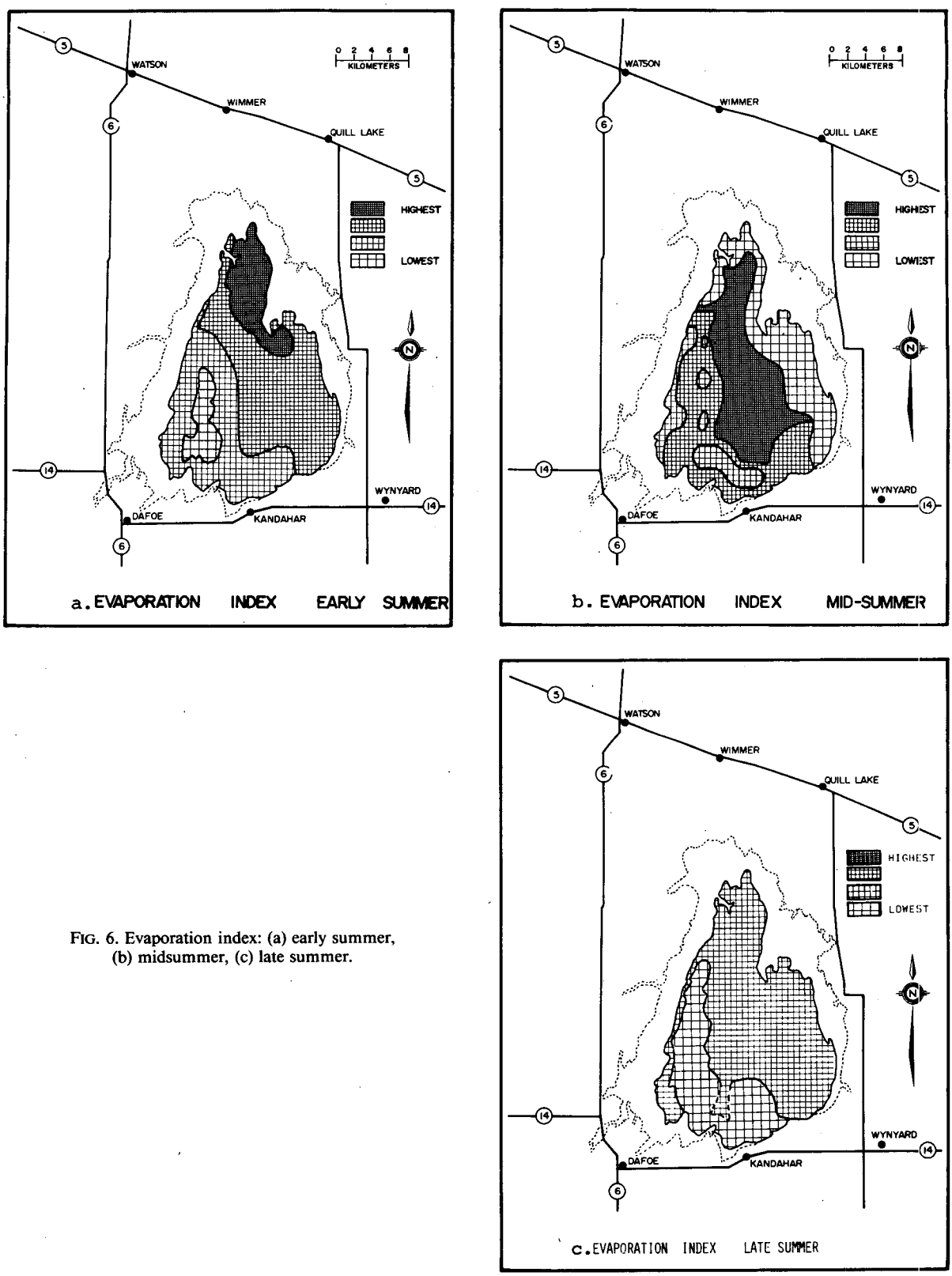

FIG. 6. Evaporation index: (a) early summer, (b) midsummer, (c) late summer.

groundwater inflows are not included in evaporation calculations. In most water balance calculations, any errors are assigned to the groundwater parameter (Wartena, 1974). The method described reduces the error assigned to the groundwater. The method also determines if the groundwater is a constant source

which further reduces errors in water balance calculations.

Acknowledgments. This project was financed by the Saskatchewan Research Council and the Canada Centre for Inland Waters (DSS contract KW 111-2-1077). Equipment was also supplied by the Atmospheric Environment Service and the Canada Centre for Remote Sensing. The author also acknowledges the work of Earl Christiansen and W. A. Meneley in the drilling program and identification of aquifers surrounding the lake.

REFERENCES

Banks, R. B., 1975: Some features of wind action on shallow lakes. *J. Environ. Eng. Div., ASCE,* **EE5,** 813–827.

Bukata, R. P., and J. E. Bruton, 1974: ERTS-1 Digital classification of the water regimes comprising Lake Ontario. *Proc. Second Can. Symp. on Remote Sensing,* Ottawa, Can. Remote Sensing Soc., Can. Aeronaut. and Space Inst., **2,** 627.

Lakshman, G., 1972: An aerodynamic formula to compute evaporation from open water surfaces. *J. Hydrol.,* **15,** 209–225.

Lee, K., 1969: IR exploration for shoreline springs at Mono Lake, Calif. test site. *Proc. Sixth Int. Symp. on Remote Sensing of Environ.,* **2,** 1075–1100.

McLin, S. G., M. A. Reiter and A. R. Sanford, 1975: Measurement of the horizontal component of groundwater flow using a vertical positioned *in-situ* thermal probe. New Mexico Water Resources Inst. Tech. Rep., A-044-NMEX., 34 pp. [NTIS PB-242 312/7].

Otterman, J., and R. S. Frazer, 1976: Earth atmospheric systems and surface reflectivities in arid regions from LANDSAT MSS data. *Remote Sens. Environ.,* **5,** 256–262.

Penman, H. L., 1948: Natural evaporation. *Proc. Roy. Soc. London,* **A193,** 120–145.

Wartena, L., 1974: Basic difficulties in predicting evaporation. *J. Hydrol.,* **23,** 159–177.

Whiting, J. M., 1976: Determination of groundwater inflow to prairie lakes using remote sensing. *IEEE Trans. on Geosci. Electron.,* **GE-14,** 60–65.

——, 1977: Hydrological and Chemical Balance of Big Quill Lake. Eng. Div., Sask. Res. Council, Saskatoon, Sask., Canada, S7N 0X1, 97 pp.

Wu, J., 1973: Prediction of near-surface drift currents from wind velocity. *J. Hydraul. Div., Amer. Soc. Civ. Eng.,* **99** (HY9), 1291–1302.